 doi:10.20944/preprints201910.0108.v1

Investigation of the effects of steam injection on equilibrium products and thermodynamic properties of diesel and biodiesel fuels

Jean Paul Gram Shou[a,*], Marcel Obounou[a], Timoléon Crépin Kofané[b], Mahamat Hassane Babikir[a]

[a] *Laboratory of Energy and Electrical Systems and Electronics, Department of Physics, Faculty of Science*
University of Yaoundé I, Yaoundé, Cameroon
P.O.Box: 812 - Yaoundé, Cameroon
[b] *Laboratory of Mechanics, Materials and Structures, Department of Physics, Faculty of Science*
University of Yaoundé I, Yaoundé, Cameroon
P.O.Box: 812 - Yaoundé, Cameroon

Abstract

The use of biodiesel fuels in compression ignition engines leads to decrease CO, PM, HC and smoke opacity. However, NO_x emissions increase importantly. Various methods to reduce NO_x are used namely the EGR, the water injection method and the steam injection method. In this study, the steam injection method has been used instead of the other methods because of its benefits. This study examines the effects of steam injection on combustion products of diesel and biodiesel fuels by considering chemical equilibrium in order to determine the equilibrium combustion products involving 10 combustion products. A developed simulation code determing the equilibrium mole fractions and thermodynamic properties of combustion products is used for diesel and biodiesel fuels. It can be used for any fuel consisting of carbon, hydrogen or any oxygenated fuel. The results show that the mole fraction of CO_2 and CO decrease with the steam injection ratios. NO mole fractions decrease with steam injection for lean mixtures but they increase slightly in the case of rich mixtures. The specific heat of combustion products increase with the steam injection ratios. Thus, the engine performance can be improved using the method. The model has been validated by comparing model results with the ones of NASA CEA software and GASEQ software using the methane as fuel. The relative errors of equilibrium mole fractions and thermodynamic properties of combustion products are less than 0.98 %.

Keywords: Chemical equilibrium products, combustion, biodiesel, diesel, steam injection method.

1. Introduction

Petroleum products are the main sources of energy for internal combustion engines in the world in general and in Cameroon in particular. However, combustion in internal combustion engines is a major source of pollutant emissions. More severe environmental restrictions have been put into effect in many countries worldwide due to the growing concern about environmental issues. In addition, the use of fossil fuels is still dominant in almost all internal combustion engines despites the fact that the resources of the fossil fuels are depleting rapidly. Thus, researchers carry out studies on combustion in internal combustion engines and alternative fuels. In this regard, biodiesels could be considered as an alternative fuels to fossil fuels to meet the growing fuel demand and the severe environmental requirements. The biodiesel properties are very close to the ones of diesel. However, the drawbacks of biodiesels are higher viscosity, lower energy content, higher cloud point and pour point, higher nitrogen oxides emissions, injector coking, engine compatibility, and higher engine wear [1]. The differences in chemical properies of fuels affect the combustion process development which lead to the alteration of performance and emissions of engine [2]. Biodiesels are formed from many different classes of saturated and unsaturated fatty acids which form their physical and chemical properties [3]. Biodiesel combustion is difficult to model because of the diversity of its sources and complexity in molecular structure [4–8].

Chemical equilibrium model is a better estimation for a combustion model assuming that the combustion products are at a chemical equilibrium in a high temperature combustion. The combustion products react together to produce and remove each species at equal rates consequently the net change in species composition remains constant at a given condition [9]. Chemical equilibrium models are used in thermodynamic simulations of internal combustion engines [10, 11]. A simple model including only six species of the products, namely CO_2, H_2O, N_2, O_2, CO, H_2, has been defined by Heywood [12]. Gonca [13] investigated the effects of steam injection on performance and NO emissions of a diesel engine running with ethano-diesel blend. In their study, various ethano-diesel blends were evaluated depending on their steam/air ratios by means of constituted solving schema based on chemical equilibrium. Abbe et al.[14] carried out a numerical study to compare four biodiesel surrogates using a zero-dimensional thermodynamic model in-

*Principal corresponding author. Tel.:+237 695 02 02 22
Email addresses: jpgram@uy1.uninet.cm (Jean Paul Gram Shou), marcelobounou@yahoo.fr (Marcel Obounou), tckofane@yahoo.com (Timoléon Crépin Kofané), hassanemahamat6@gmail.com (Mahamat Hassane Babikir)

Preprints (www.preprints.org) | NOT PEER-REVIEWED | Posted: 10 October 2019 doi:10.20944/preprints201910.0108.v1

volving a chemical equilibrium combustion model. A chemical equilibrium model was used by Ust and Kayadelen [15]. 10 combustion products were used to predict their equilibrium and thermodynamic properties in a H_2O injected combustion system at various H_2O rates. They neglected the CO and H_2 formations in lean mixtures. They formed their equation systems for lean and rich mixtures separately. Rakopoulos et al.[16] performed a two-zone thermodynamic model for combustion and emissions formation in a direct injection diesel engine. They used a chemical equilibrium scheme involving 11 species of combustion products for calculating the constituents in exhaust gases. Diotallevi [17] developed a multi-zone thermodynamic model of a diesel engine for NO_x formation. He created a chemical equilibrium scheme by considering 10 combustion products. The nonlinear system of equations created was solved using an iterative method developed by the author using the Matlab program. Mourya and Roy [18] performed a study on the combustion modelling of a diesel engine operating using jatropha biodiesel and diesel engine blends according to a chemical equilibrium model. The C program and Mathematica software developed by the authors were used to solve their equations. Kayadelen [19] developed a multi-featured model for estimation of the mole fractions of 14 equilibrium combustion products, thermodynamic properties and adiabatic flame temperature of fuels, surrogates and fuel additives. He constituted his equation systems for lean and rich mixtures separately. CO and H_2 mole fractions were neglected in lean mixtures. The nonlinear equation systems were solved using both Newton-Raphson and Gauss-Seidel methods.

Some equilibrium computer programs exist like GASEQ [20] and CEA of NASA [21]. However, GASEQ software neglects effects of dissociations on the specific heat of the combustion products. Consequently, noticeable error may be resulted in engines performance calculations. In the other hand, CEA of NASA necessitates adiabatic flame temperature or enthalpy of combustion to be given. Important differences are reported between the specific heat results of GASEQ and CEA of NASA particularly at high temperature. The present model takes into account the effect of combustion products dissociations with temperature on specific heat of the gas mixture. The adiabatic flame temperature or combustion enthalpy is not needed as input but they can be calculated by the model.

The objective of this study is to validate the model with the above mentioned range of computer programs and compare the equilibrium mole fractions and thermodynamic properties of combustion products of diesel with thz ones of biodiesel. For this purpose, the solving schema of the combustion model based on a chemical equilibrium was developed for biodiesel and diesel fuels. The nonlinear system of equations are solved using Newton-Raphson and Gauss-Seidel methods. The diesel and biodiesels with chemical compositions $C_{14.09}H_{24.78}$ [22], $C_{18.74}H_{34.43}O_2$ [22] and $C_{18}H_{36}O_2$ [23] were used to represent diesel and biodiesel fuels respectively.

2. Theoretical equilibrium combustion products model

2.1. Equilibrium combustion products

The combustion products are supposed to be consisted of ten species which are all assumed as ideal gases and they are defined by dissociation considerations as follows [24]:

$$\frac{1}{2}H_2 \rightleftharpoons H \qquad K_1 = \frac{x_7 p^{1/2}}{x_6^{1/2}} \tag{1}$$

$$\frac{1}{2}O_2 \rightleftharpoons O \qquad K_2 = \frac{x_8 p^{1/2}}{x_4^{1/2}} \tag{2}$$

$$\frac{1}{2}H_2 + \frac{1}{2}O_2 \rightleftharpoons OH \qquad K_3 = \frac{x_9}{x_4^{1/2} x_6^{1/2}} \tag{3}$$

$$\frac{1}{2}O_2 + \frac{1}{2}N_2 \rightleftharpoons NO \qquad K_4 = \frac{x_{10}}{x_3^{1/2} x_4^{1/2}} \tag{4}$$

$$H_2 + \frac{1}{2}O_2 \rightleftharpoons H_2O \qquad K_5 = \frac{x_2}{x_4^{1/2} x_6 p^{1/2}} \tag{5}$$

$$CO + \frac{1}{2}O_2 \rightleftharpoons CO_2 \qquad K_6 = \frac{x_1}{x_4^{1/2} x_5 p^{1/2}} \tag{6}$$

where the unit of pressure p is in atmospheres and K_1 to K_6 are the equilibrium constants of the reactions. Olikara and Borman [25] have curve fitted the equilibrium constants K_i to JANAF Table data for the temperature between 600K and 4000K and its values are calculated by using Eq.(7).

$$\log K_i = A_i \ln(\frac{T}{1000}) + \frac{B_i}{T} + C_i + D_i T + E_i T^2 \tag{7}$$

where the equilibrium constant curve-fit coefficients A_i, B_i, C_i, D_i and E_i are listed in Table 1 presented by Ferguson [24].

2.2. Equilibrium combustion model

2.2.1. Low-temperature products

At low temperatures ($T < 1000K$) and for α/γ ratios less than one, the overall chemical reactions which describe the combustion ($\phi < 3$) are given below:

$$\varepsilon\phi C_\alpha H_\beta O_\gamma N_\delta + (0.21O_2 + 0.79N_2) \rightarrow \nu_1 CO_2 + \nu_2 H_2O + \nu_3 N_2 + \nu_4 O_2 + \nu_5 CO + \nu_6 H_2 \tag{8}$$

For the lean and stoichiometric combustion, it is assumed that there would be enough oxygen to oxidize all CO and H_2 that means CO and H_2 are negligible. It can be noticed that the equilibrium composition is independent from the temperature and pressure. It only depends on equivalence ratio ϕ. The product composition is determined using atom balance equations. Products of wet combustion for the low temperature are give in the Table 2.

For the rich case, it is assumed that there is insufficient oxygen to oxidize all CO and H_2 that means all the oxygen is consumed. When writing atom balances, five unknowns and four equations are found. One more equation Eq.(10) is used and it depends on the equilibrium constant for the water-gas reaction

Preprints (www.preprints.org) | NOT PEER-REVIEWED | Posted: 10 October 2019 doi:10.20944/preprints201910.0108.v1

Table 1: Olikara and Borman equilibrium constant curve-fit coefficients

i	A_i	B_i	C_i	D_i	E_i
1	0.432168	-0.112464×10^5	0.267269×10^1	-0.745744×10^{-4}	0.242484×10^{-8}
2	0.310805	-0.129540×10^5	0.321779×10^1	-0.738336×10^{-4}	0.344645×10^{-8}
3	−0.141784	-0.213308×10^4	0.853461	0.355015×10^{-4}	-0.310227×10^{-8}
4	0.150879×10^{-1}	-0.470959×10^4	0.646096	0.272805×10^{-5}	-0.154444×10^{-8}
5	−0.752364	0.124210×10^5	-0.260286×10^1	0.259556×10^{-3}	-0.162687×10^{-7}
6	-0.415302×10^{-2}	0.148627×10^5	-0.475746×10^1	0.124699×10^{-3}	-0.900227×10^{-8}

Table 2: Products of wet combustion for T< 1000K

i	Species	$\phi \leq 1$	$\phi > 1$
1	CO_2	$\alpha\phi\varepsilon$	$\alpha\phi\varepsilon - \nu_5$
2	H_2O	$\beta\phi\varepsilon + x$	$\phi\varepsilon(\gamma - 2\alpha) + 0.42 + \nu_5$
3	N_2	$0.79 + \delta\phi\varepsilon/2$	$0.79 + \delta\phi\varepsilon/2$
4	O_2	$0.21(1 - \phi)$	0
5	CO_2	0	ν_5
6	H_2	0	$0.42(\phi) - 1) - \nu_5$

given by Ferguson [20] for the range of temperatures between 400K and 3200K.

$$\ln K = 2.743 - \frac{1.761}{t} - \frac{1.611}{t^2} + \frac{0.2803}{t^3} \tag{9}$$

where t=T/1000.

The equilibrium constant at constant pressure K of the water-gas reaction is expressed as follows:

$$CO_2 + H_2 \rightleftharpoons CO + H_2O \qquad K = \frac{\nu_2\nu_5}{\nu_1\nu_6} \tag{10}$$

2.2.2. High-temperature products

At higher temperatures ($T \geq 1000K$) and for α/γ ratios less than one, the overall chemical reactions which describe the combustion ($\phi < 3$) are given below:

$$\begin{aligned} \varepsilon\phi C_\alpha H_\beta O_\gamma N_\delta + (0.21O_2 + 0.79N_2) + xH_2O \rightarrow \nu_1 CO_2 \\ +\nu_2 H_2O + \nu_3 N_2 + \nu_4 O_2 + \nu_5 CO + \nu_6 H_2 \\ +\nu_7 H + \nu_8 O + \nu_9 OH + \nu_{10} N \end{aligned} \tag{11}$$

where ν_i denotes the number of moles for each product, α, β, γ and δ represent the atom numbers of carbon, hydrogen, oxygen and nitrogen in the used fuel respectively. For diesel fuel γ and δ are zeroes.

When the product mole fraction composition is known at given temperature, equivalence ratio, and pressure, the thermodynamic properties of interest such as enthalpy, entropy, specific volume, and internal energy can be computed.

The atom balance for various elements in Eq.(11), the constraint that the mole fraction of all the products adds up to one, the unknown total product moles N and the six dissociation equations provided by the criteria of equilibrium among combustion products Eqs.(1)-(6) yield to 11 equations for 11 unknowns namely unknown mole fractions x_i and the unknown total product moles N. After writing the mole fractions of the other combustion species with respect to the mole fractions of four independent variables x_3, x_4, x_5 and x_6, the following non-linear equations are obtained.

$$\begin{aligned} f_1 = C_6 x_4^{1/2} x_5 + C_5 x_4^{1/2} x_6 + x_3 + x_4 + x_5 + x_6 + C_1 x_6^{1/2} \\ +C_2 x_4^{1/2} + C_3 x_4^{1/2} x_6^{1/2} + C_4 x_3^{1/2} x_4^{1/2} - 1 = 0 \end{aligned} \tag{12}$$

$$\begin{aligned} f_2 = 2C_5 x_4^{1/2} x_6 + 2x_6 + C_1 x_6^{1/2} + C_3 x_4^{1/2} x_6^{1/2} \\ -d_1(C_6 x_4^{1/2} x_5 + x_5) = 0 \end{aligned} \tag{13}$$

$$\begin{aligned} f_3 = 2C_6 x_4^{1/2} x_5 + C_5 x_4^{1/2} x_6 + 2x_4 + x_5 + C_2 x_4^{1/2} \\ +C_3 x_4^{1/2} x_6^{1/2} + C_4 x_3^{1/2} x_4^{1/2} - d_2(C_6 x_4^{1/2} x_5 + x_5) = 0 \end{aligned} \tag{14}$$

$$f_4 = 2x_3 + C_4 x_3^{1/2} x_4^{1/2} - d_3(C_6 x_4^{1/2} x_5 + x_5) = 0 \tag{15}$$

where

$$C_1 = \frac{k_1}{p^{1/2}} \tag{16}$$

$$C_2 = \frac{k_2}{p^{1/2}} \tag{17}$$

$$C_3 = K_3 \tag{18}$$

$$C_4 = k_4 \tag{19}$$

$$C_5 = k_5 p^{1/2} \tag{20}$$

$$C_6 = K_6 p^{1/2} \tag{21}$$

$$d_1 = \frac{\varepsilon\phi\beta + 2x}{\varepsilon\phi\alpha} \tag{22}$$

$$d_2 = \frac{\varepsilon\phi\gamma + 0.42 + x}{\varepsilon\phi\alpha} \tag{23}$$

$$d_3 = \frac{\varepsilon\phi\delta + 1.58}{\varepsilon\phi\alpha} \tag{24}$$

Preprints (www.preprints.org) | NOT PEER-REVIEWED | Posted: 10 October 2019 doi:10.20944/preprints201910.0108.v1

The equivalence ratio ϕ and the molar fuel/air ratio ε are expressed as follows:

$$\phi = \frac{m_f/m_a}{(m_f/m_a)_s} \tag{25}$$

$$\varepsilon = \frac{0.21}{\alpha - \frac{\gamma}{2} + \frac{\beta}{4}} \tag{26}$$

By setting a vector for unknowns $x = (x_3, x_4, x_5, x_6)^T$, the correction vector $\delta x = (\delta x_3, \delta x_4, \delta x_5, \delta x_6)^T$, and f_3, f_4, f_5, f_6 the coordinate functions of F.

$$F(x) = [f_3, f_4, f_5, f_6] = 0 \tag{27}$$

If the exact solution of the problem is $x = x^{(0)} + \delta x$ which means:

$$F(x^{(0)} + \delta x) = 0 \tag{28}$$

where $x^{(0)}$ is a given rough initial guess and δx is the correction term. In the neighbourhoods of $x^{(0)}$, each of the coordinate function of F can be expanded in Taylor series, truncated after the first derivative. We obtain a set of linear equations for the correction δx that move each function closer to zero simultaneously.

$$\mathfrak{J}(x^{(0)})\delta x = -F(x^{(0)}) \tag{29}$$

The Jacobian matrix $\mathfrak{J}$ is expressed as

$$\mathfrak{J}(x^{(0)}) = \begin{pmatrix} \frac{\partial f_1(x^{(0)})}{\partial x_3} & \frac{\partial f_1(x^{(0)})}{\partial x_4} & \cdots & \frac{\partial f_1(x^{(0)})}{\partial x_6} \\ \frac{\partial f_2(x^{(0)})}{\partial x_3} & \frac{\partial f_2(x^{(0)})}{\partial x_4} & \cdots & \frac{\partial f_2(x^{(0)})}{\partial x_6} \\ \vdots & \vdots & \ddots & \vdots \\ \frac{\partial f_4(x^{(0)})}{\partial x_3} & \frac{\partial f_4(x^{(0)})}{\partial x_4} & \cdots & \frac{\partial f_4(x^{(0)})}{\partial x_6} \end{pmatrix}$$

The set of linear equations Eq.(29) is solved for δx using Gauss-Seidel iterative method. The new approximated solution is calculated as $x^{(1)} = x^{(0)} + \delta x$.

If $x^{(1)}$ does not approximate the solution to the given tolerance, a new correction term is calculated as follows:

$$\mathfrak{J}(x^{(k)})\delta x^{(k)} = -F(x^{(k)}) \tag{30}$$

The procedure is repeated until δx reaches a specified tolerance which leads to the values for x_3, x_4, x_5 and x_6. The other dependent unknowns are expressed after determing the mole fractions x_3, x_4, x_5 and x_6 as follows:

$$x_1 = C_6 x_4^{1/2} x_5 \tag{31}$$

$$x_2 = C_5 x_4^{1/2} x_6 \tag{32}$$

$$x_7 = C_1 x_6^{1/2} \tag{33}$$

$$x_8 = C_2 x_4^{1/2} \tag{34}$$

$$x_9 = C_3 x_4^{1/2} x_6^{1/2} \tag{35}$$

$$x_{10} = C_4 x_3^{1/2} x_4^{1/2} \tag{36}$$

2.3. Thermodynamic properties

At constant pressure, temperature variation has effect on specific heat due to the dissociations of species at high temperature. The effect of temperature on mole fractions should be considered during the equilibrium specific heat calculation differentiating with respect to temperature written as:

$$\mathfrak{J}(x^{(k)})x_T^{(k)} = -F_T(x^{(k)}) \tag{37}$$

where

$$F_T = \frac{\partial F}{\partial T} \qquad and \qquad x_T = \frac{\partial x}{\partial T} \tag{38}$$

The same procedure is used to solve Eq.(37). The results are used in computing the specific heat of the gas mixture in Eq.(44).

Gordon and McBride [26] proposed the expressions of molar specific heat at constant pressure $\bar{c}_{p,i}$, enthalpy $\bar{h}_i^0$ and entropy $\bar{s}_i^0$ values of each species that were curve-fitted to the tabulated JANAF Thermochemical tables [27].

At constant pressure, enthalpy of the gas mixture $\bar{h}$ change due to the dissociations because the mole fractions of the species change with temperature.

$$\bar{h} = \sum_{i=1}^{10} x_i \bar{h}_i^0 \tag{39}$$

$$\bar{s} = \sum_{i=1}^{10} R_u x_i \left(\frac{\bar{s}_i^0}{R_u} - \ln\left(\frac{x_i p}{p_0}\right) \right) \tag{40}$$

$$M = \sum_{i=1}^{10} x_i M_i \tag{41}$$

$$h = \frac{1}{M} \sum_{i=1}^{10} x_i \bar{h}_i^0 \tag{42}$$

$$s = \frac{R_u}{M} \sum_{i=1}^{10} x_i \left(\frac{\bar{s}_i^0}{R_u} - \ln\left(\frac{x_i p}{p_0}\right) \right) \tag{43}$$

$$c_p = \left(\frac{\partial h}{\partial T}\right)_p = \frac{1}{M} \sum_{i=1}^{10} \left(x_i \bar{c}_{p,i} + \bar{h}_i^0 \frac{\partial x_i}{\partial T} - \frac{M_T}{M} x_i \bar{h}_i^0 \right) \tag{44}$$

where

$$M_T = \frac{\partial M}{\partial T} = \sum_{i=1}^{10} M_i \frac{\partial x_i}{\partial T} \tag{45}$$

2.4. Validation of the model

The validation of the model is done by comparing the model results with the results of software CEA [21] and software GASEQ [20] which use element potential method and minimization of Gibbs free energy approach respectively. The simulations of methane with steam injection are conducted.

Preprints (www.preprints.org) | NOT PEER-REVIEWED | Posted: 10 October 2019 doi:10.20944/preprints201910.0108.v1

Table 3: Comparison of the present model results with the ones obtained from CEA and GASEQ software for equilibrium combustion products of methane at $\phi = 0.6$ and steam injection 10 %

ϕ=0.6	Model results	GASEQ results	CEA results	GASEQ relative error (%)	CEA relative error (%)
CO_2	0.051506	0.05154	0.05151	0.066	0.066
H_2O	0.233920	0.23399	0.23385	0.029	0.029
N_2	0.645559	0.64553	0.64553	−0.005	−0.005
O_2	0.068353	0.06827	0.06827	−0.122	−0.122
CO	1.328×10^{-7}	1.33×10^{-7}	3.27×10^{-7}	−0.157	−0.157
H_2	2.419×10^{-7}	2.41×10^{-7}	2.41×10^{-7}	−0.360	−0.360
H	1.269×10^{-9}	1.27×10^{-9}	1.27×10^{-9}	0.03	0.03
O	1.506×10^{-7}	1.50×10^{-7}	1.50×10^{-7}	−0.429	−0.429
OH	3.263×10^{-5}	3.39×10^{-5}	3.39×10^{-5}	3.751	3.751
NO	6.278×10^{-4}	6.27×10^{-4}	6.27×10^{-4}	−0.126	−0.126
C_p	1.46488	1.45383	1.45383	−0.76	−0.76
T_{in}	300	300	300	0.000	0.000
T_{ad}	1482.3	1482.3	1482.3	0.000	0.000

Table 4: Comparison of the present model results with the ones obtained from CEA and GASEQ software for equilibrium combustion products of methane at $\phi = 1.2$ and steam injection 10 %

ϕ=1.2	Model results	GASEQ results	CEA results	GASEQ relative error (%)	CEA relative error (%)
CO_2	0.063729	0.06368	0.06368	−0.077	−0.077
H_2O	0.278173	0.27822	0.27822	0.017	0.017
N_2	0.594799	0.59480	0.59480	0.00017	0.00017
O_2	5.826×10^{-8}	5.78×10^{-8}	5.78×10^{-8}	−0.790	−0.790
CO	0.031138	0.03119	0.03119	0.168	0.168
H_2	0.032106	0.03206	0.03206	−0.144	−0.144
H	2.988×10^{-5}	2.98×10^{-5}	2.98×10^{-5}	−0.260	−0.260
O	1.535×10^{-8}	1.53×10^{-8}	1.53×10^{-8}	−0.345	−0.345
OH	2.199×10^{-5}	2.95×10^{-6}	2.68×10^{-6}	2.679	2.57
NO	2.962×10^{-6}	2.95×10^{-6}	0.646096	−0.394	−0.394
C_p	1.64592	1.63042	1.63042	−0.95	−0.95
T_{in}	300	300	300	0.000	0.000
T_{ad}	1919.3	1919.3	1919.3	0.000	0.000

Preprints (www.preprints.org) | NOT PEER-REVIEWED | Posted: 10 October 2019 doi:10.20944/preprints201910.0108.v1

3. Results and discussion

3.1. Mole fraction of combustion products

Adiabatic combustion simulation with steam has been carried out for the biodiesel and diesel fuels in order to investigate the effects of steam injection on the equilibrium combustion products and thermodynamic properties. The results have been comparatively presented for lean and rich combustion with increasing steam injection from 0% to 10%.

Figure 1 shows the CO_2 equilibrium mole fractions with steam injection ratios and they decrease remarkably with increasing steam injection ratios. NBD gives the highest results while WCOBD presents the lowest results. This trend can be explained by the α/β ratio and the different stoichiometric air/fuel ratios.

Figure 2 illustrates the H_2O equilibrium mole fractions with steam injection ratios. It is clear that the H_2O equilibrium mole fraction increases with increasing steam injection ratios. The maximum H_2O equilibrium mole fraction is obtained with WCOBD and the minimum H_2O equilibrium mole fraction is observed with diesel fuel. The reason is the WCOBD has the lowest α/β ratio and diesel fuel has the highest α/β ratio.

Figure 3 illustrates the N_2 equilibrium mole fractions with steam injection ratios. It is clear that the N_2 equilibrium mole fraction decreases with increasing steam injection ratios. The maximum N_2 equilibrium mole fraction is obtained with diesel fue and the minimum N_2 equilibrium mole fraction is observed with lWCOBD. The reason is the WCOBD has the lowest α/β ratio and diesel fuel has the highest α/β ratio.

Figure 4 shows the O_2 equilibrium mole fractions with steam injection ratios. It is clear that the O_2 equilibrium mole fraction decreases with increasing steam injection ratios in the case of lean combustion. The maximum O_2 equilibrium mole fraction is obtained with diesel fuel and the minimum O_2 equilibrium mole fraction is observed with WCOBD. The O_2 equilibrium mole fractions is much lower in rich combustion due to lower oxygen concentration compared to lean combustion. The maximum O_2 equilibrium mole fraction happens with WCOBD and the minimum O_2 equilibrium mole fractions occurs with diesel fuel. The influence of the steam injection has the similar trend in Figure 8.

Figure 5 shows the CO equilibrium mole fractions with steam injection ratios. The CO equilibrium mole fraction decreases with increasing steam injection ratios. The maximum CO equilibrium mole fraction is obtained with diesel fuel and the minimum CO equilibrium mole fraction is observed with WCOBD in the case of rich combustion. The maximum CO equilibrium mole fraction is obtained with NBD and the minimum CO equilibrium mole fraction is observed with WCOBD in the case of lean combustion. The O_2 equilibrium mole fractions is much lower in rich combustion due to lower oxygen concentration compared to lean combustion. The maximum O_2 equilibrium mole fraction happens with WCOBD and the minimum O_2 equilibrium mole fractions occurs with diesel fuel.

Figure 6 shows the H_2 equilibrium mole fractions with steam injection ratios which increase in both rich and lean combustions. The combustion of WCOBD gives the highest H_2 equilibrium mole fraction. The influence of the steam injection has the similar trend in Figure 7.

Figure 9 demonstrates the OH equilibrium mole fractions with steam injection ratios. The OH equilibrium mole fractions increase slightly with increasing steam injection ratios in rich and lean combustion. WCOBD releases the highest OH equilibrium mole fractions while diesel fuel releases the lowest OH equilibrium mole fractions in both rich and lean combustions.

Figure 10 demonstrates the NO equilibrium mole fractions with steam injection ratios. The NO equilibrium mole fractions decrease with increasing steam injection ratios in lean combustion. Diesel fuel releases the highest NO equilibrium mole fractions while WCOBD releases the lowest NO equilibrium mole fractions in lean combustions.

3.2. Thermodynamic properties of combustion products

The specific heat and the enthalpy of the mixture gases increase with the steam injection ratios due to the specific of superheated steam which is higher than the one of the air at that condition temperature.

Figures 11 shows the average specific heats with respect to steam injection ratios. Higher specific heats are obtained in the rich combustions compared to lean combustions. The highest specific heats are seen with WCOBD and the lowest specific heats are obtainded with diesel fuel. In both combustions, specific heats increase with increasing steam injection ratios . Because the specific heat of the steam is much more than the ones of the combustion products at the same temperature.

Figures 12 shows the average specific heats with respect to steam injection ratios. Higher specific heats are obtained in the rich combustions compared to lean combustions. The highest specific heats are seen with WCOBD and the lowest specific heats are obtainded with diesel fuel. In both combustions, specific heats increase with increasing steam injection ratios . Because the specific heat of the steam is much more than the ones of the combustion products at the same temperature.

Figures 13 shows the average specific heats with respect to steam injection ratios. Higher specific heats are obtained in the rich combustions compared to lean combustions. The highest specific heats are seen with WCOBD and the lowest specific heats are obtainded with diesel fuel. In both combustions, specific heats increase with increasing steam injection ratios . Because the specific heat of the steam is much more than the ones of the combustion products at the same temperature.

Preprints (www.preprints.org) | NOT PEER-REVIEWED | Posted: 10 October 2019 doi:10.20944/preprints201910.0108.v1

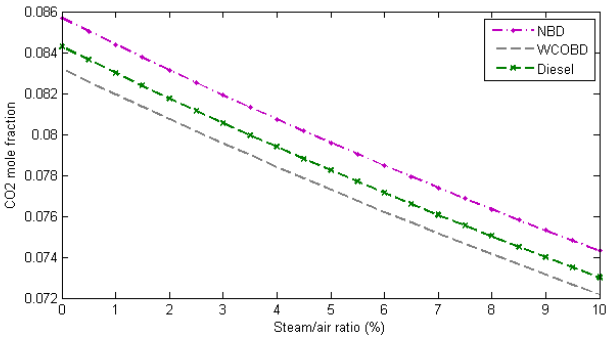

(a) $\phi = 0.6$

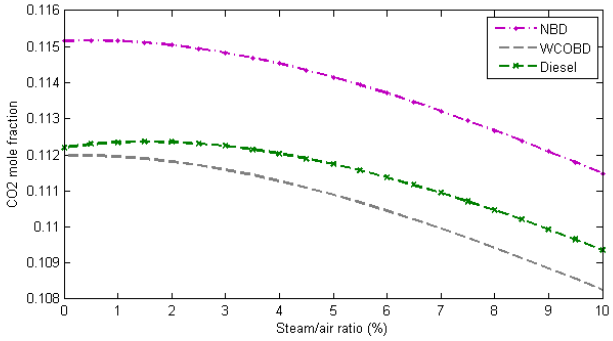

(b) $\phi = 1.2$

Figure 1: Variation of CO_2 equilibrium mole fractions with steam injection ratios

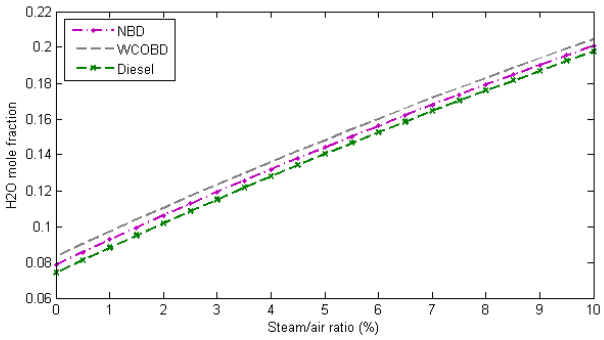

(a) $\phi = 0.6$

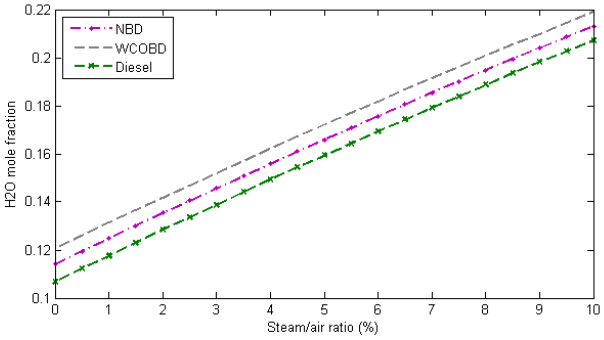

(b) $\phi = 1.2$

Figure 2: Variation of H_2O equilibrium mole fractions with steam injection ratios

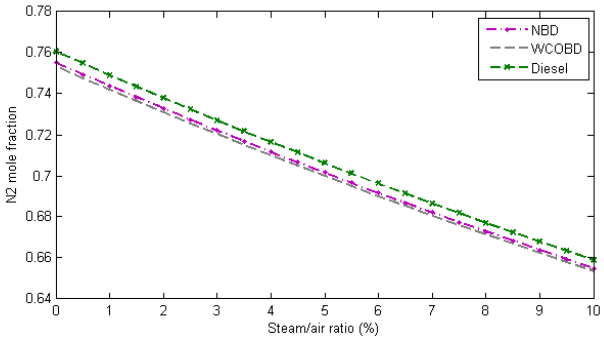

(a) $\phi = 0.6$

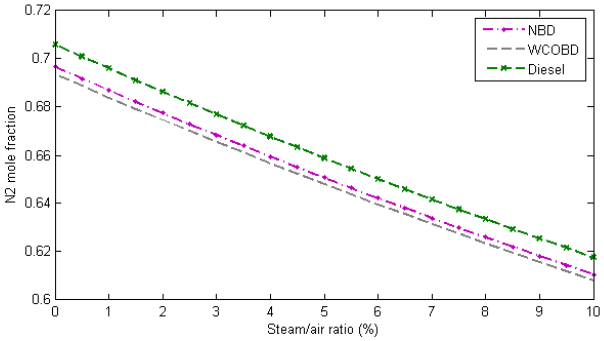

(b) $\phi = 1.2$

Figure 3: Variation of N_2 equilibrium mole fractions with steam injection ratios

Preprints (www.preprints.org) | NOT PEER-REVIEWED | Posted: 10 October 2019 doi:10.20944/preprints201910.0108.v1

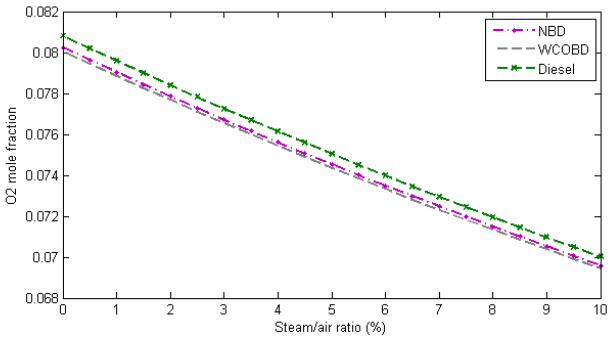

(a) $\phi = 0.6$

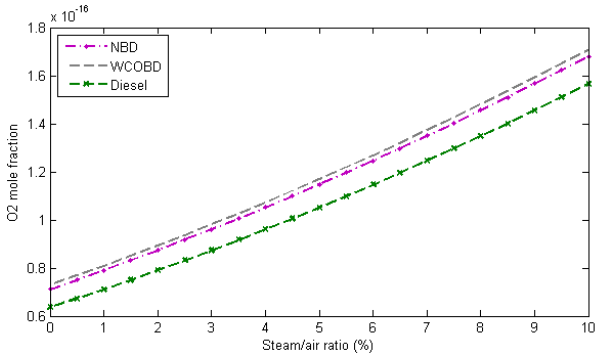

(b) $\phi = 1.2$

Figure 4: Variation of O_2 equilibrium mole fractions with steam injection ratios

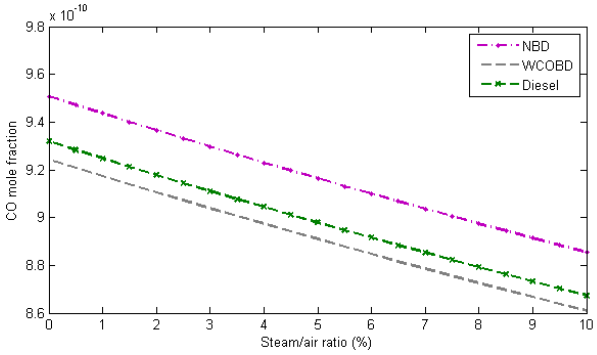

(a) $\phi = 0.6$

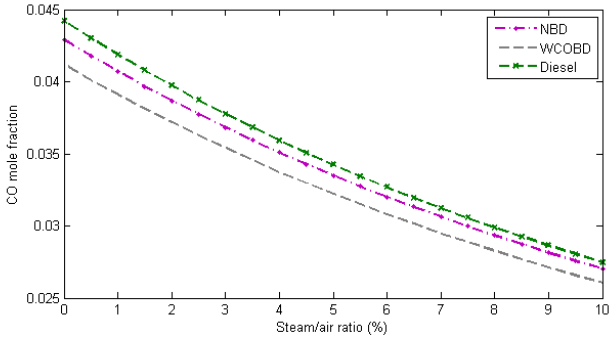

(b) $\phi = 1.2$

Figure 5: Variation of CO equilibrium mole fractions with steam injection ratios

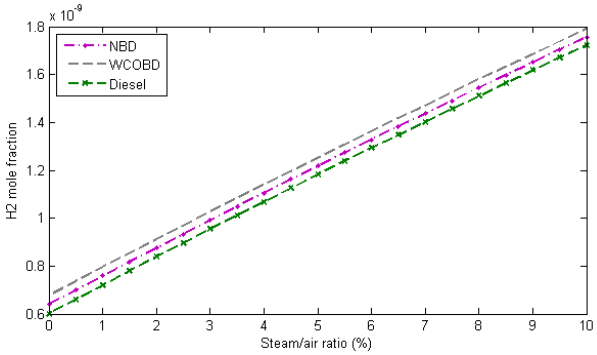

(a) $\phi = 0.6$

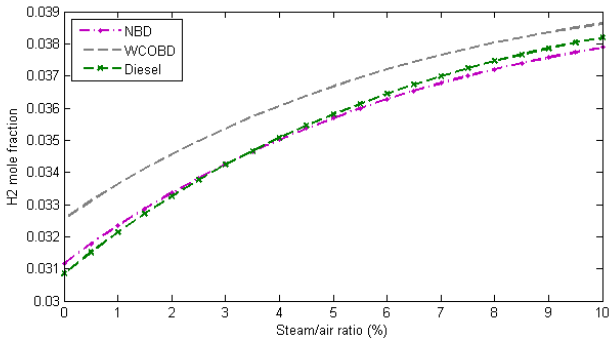

(b) $\phi = 1.2$

Figure 6: Variation of H_2 equilibrium mole fractions with steam injection ratios

Preprints (www.preprints.org) | NOT PEER-REVIEWED | Posted: 10 October 2019 doi:10.20944/preprints201910.0108.v1

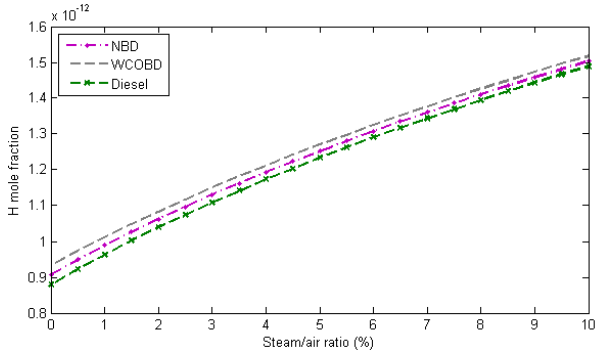

(a) $\phi = 0.6$

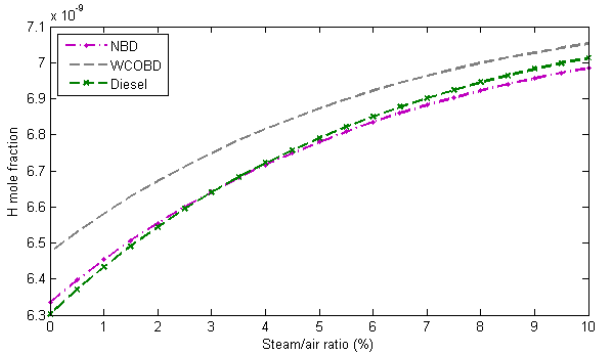

(b) $\phi = 1.2$

Figure 7: Variation of H equilibrium mole fractions with steam injection ratios

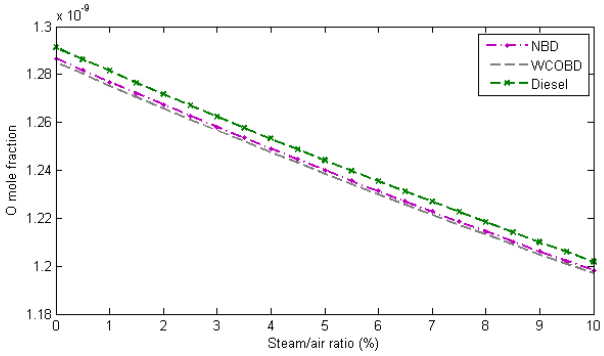

(a) $\phi = 0.6$

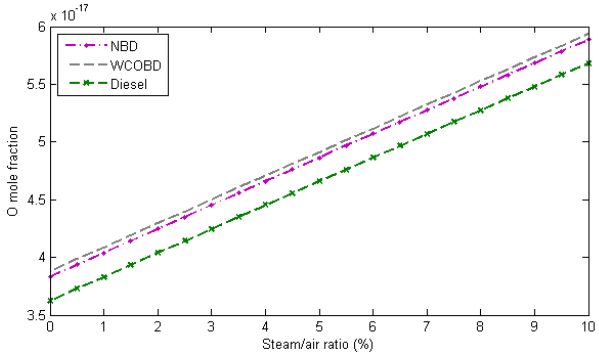

(b) $\phi = 1.2$

Figure 8: Variation of O equilibrium mole fractions with steam injection ratios

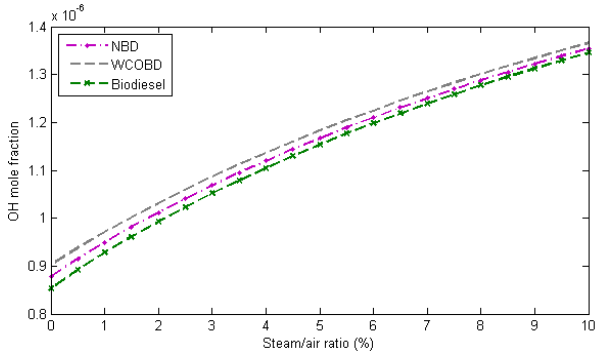

(a) $\phi = 0.6$

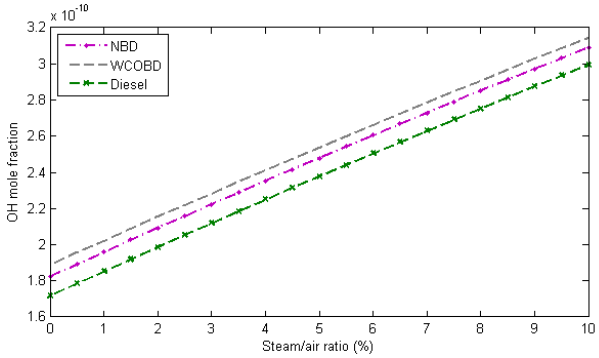

(b) $\phi = 1.2$

Figure 9: Variation of OH equilibrium mole fractions with steam injection ratios

Preprints (www.preprints.org) | NOT PEER-REVIEWED | Posted: 10 October 2019 doi:10.20944/preprints201910.0108.v1

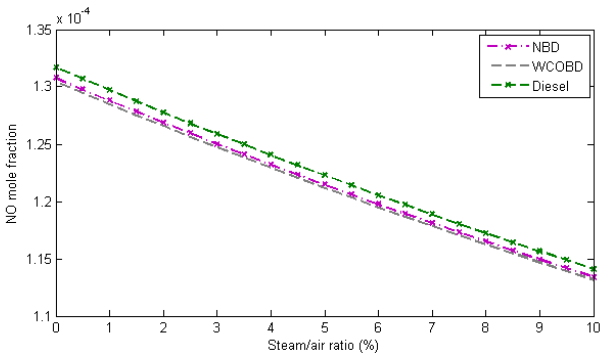

(a) $\phi = 0.6$

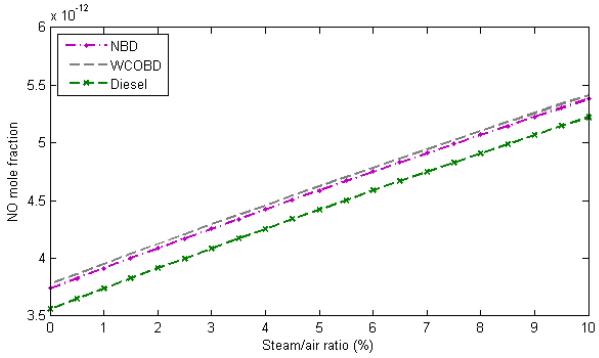

(b) $\phi = 1.2$

Figure 10: Variation of *NO* equilibrium mole fractions with steam injection ratios

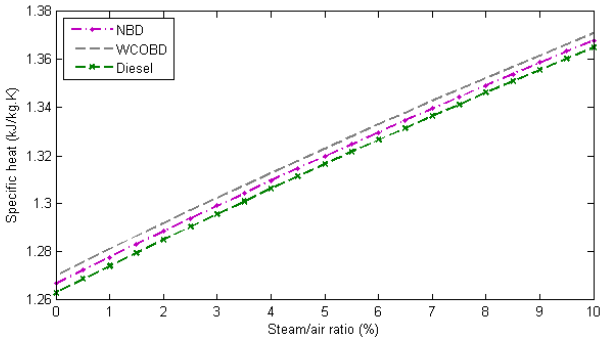

(a) $\phi = 0.6$

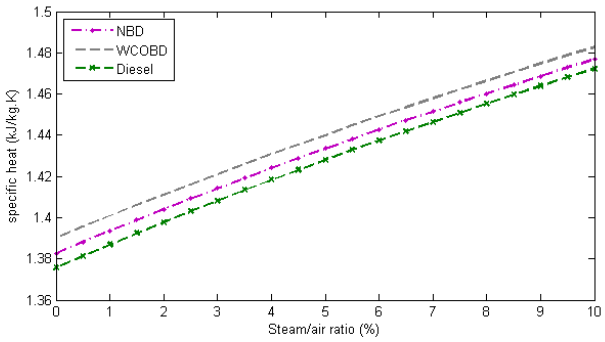

(b) $\phi = 1.2$

Figure 11: Variation of gas mixture specific heat with steam injection ratios

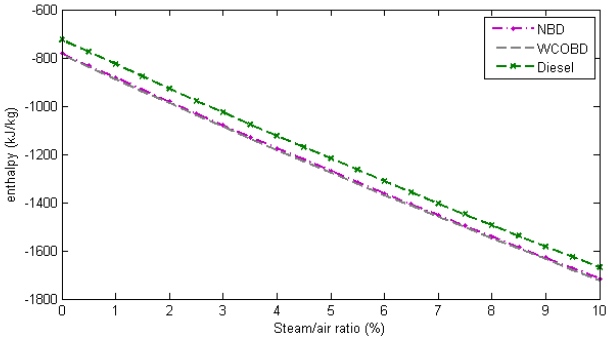

(a) $\phi = 0.6$

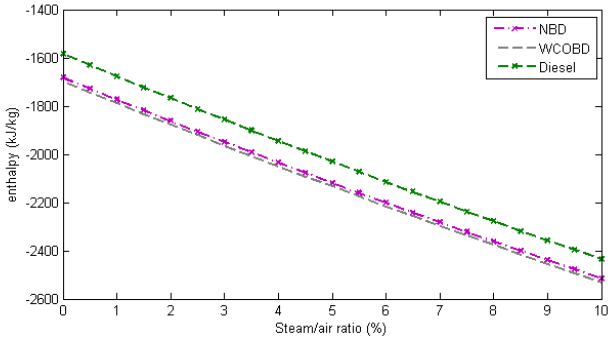

(b) $\phi = 1.2$

Figure 12: Variation of gas mixture specific heat with steam injection ratios

Preprints (www.preprints.org) | NOT PEER-REVIEWED | Posted: 10 October 2019 doi:10.20944/preprints201910.0108.v1

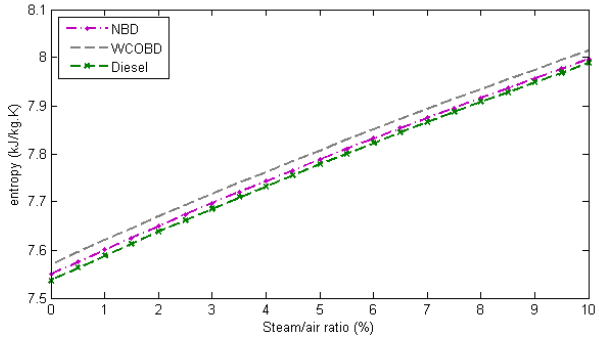

(a) $\phi = 0.6$

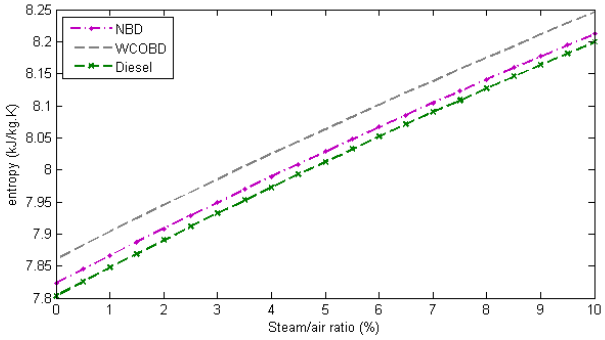

(b) $\phi = 1.2$

Figure 13: Variation of gas mixture specific heat with steam injection ratios

4. Conclusion

In this work, equilibrium combustion model is used to provide mole fractions and thermodynamic properties of combustion products in chemical equilibrium. This model can compute adiabatic flame temperature and enthalpy simultaneously with the equilibrium mole fractions of combustion products which is not the case of CEA of NASA. The influences of steam injection on equilibrium combustion products and thermodynamic properties of diesel fuel and biodiesels have been modeled. The highest CO_2 equilibrium mole fraction are seen with NBD, the lowest ones are formed with WCOBD. The reduction rate of NO is higher for biodiesels as compared to the one of diesel fuel in lean combustion conditions. Thus, the steam injection ratios can be used for biodiesels in order to lower NO equilibrium combustion products in the lean combustion conditions. Diesel engines produce more NO emissions especially when they are fuelled with biodiesel. Thus, the steam injection method could be used to decrease the NO formation. This equilibrium combustion model can be used by the researchers studying fuels and modelling internal combustion engines due to its accuracy and convenience.

Nomenclature

EGR	exhaust gas recirculation
h	specific enthalpy, $kJ.kg^{-1}$
M	molecular weight of the mixture, $kg.kmol^{-1}$
p	pressure, Pa
PM	particulate matter
s	specific entropy, $kJ.kg^{-1}.K^{-1}$
T	temperature, K
x	number of moles injected H_2O
x_i	mole fraction of species i

Greek letters

α	atomic number of carbon for fuels
β	atomic number of hydrogen for fuels
γ	atomic number of oxygen for fuels
δ	atomic number of nitrogen for fuels
ε	molar fuel-air ratio
ϕ	equivalence ratio
ν_i	number of moles for product species i

Subscripts

a	air
f	fuel
s	stoichiometric

References

[1] Demirbas A. Importance of biodiesel as transportation fuel. Energy Policy. 2007;35:4661-70.

[2] Hellier P, Talibi M, Eveleigh A, Ladommatos N. An overview of the effects of fuel molecular structure on the combustion and emissions characteristics of compression ignition engines. Proceedings of the Institution of Mechanical Engineers, Part D: Journal of Automobile Engineering. 2017:0954407016687453.

[3] Tamilselvan P, Nallusamy N, Rajkumar S. A comprehensive review on performance, combustion and emission characteristics of biodiesel fuelled diesel engines. Renewable and Sustainable Energy Reviews. 2017;79:1134-59.

[4] Coniglio L, Bennadji H, Glaude PA, Herbinet O, Billaud F. Combustion chemical kinetics of biodiesel and related compounds (methyl and ethyl esters): Experiments and modeling–advances and future refinements. Progress in Energy and Combustion Science. 2013;39:340-82.

[5] Visconti P, Primiceri P, Strafella L, Carlucci AP, Ficarella A. Morphological analysis of injected sprays of different bio-diesel fuels by using a common rail setup controlled by a programmable electronic system. International Journal of Automotive and Mechanical Engineering. 2017;14:3849-71.

[6] Nayak SK, Mishra PC. Emission from a dual fuel operated diesel engine fuelled with calophyllum inophyllum biodiesel and producer gas. International Journal of Automotive and Mechanical Engineering. 2017;14:3954-69.

[7] Shukri MR, Rahman MM, Ramasamy D, Kadirgama K. Artificial neural network optimization modeling on engine performance of diesel engine using biodiesel fuel. International Journal of Automotive and Mechanical Engineering. 2015;11:2332-47.

[8] Hasan MM, Rahman MM, Kadirgama K. A review on homogeneous charge compression ignition engine performance using biodiesel–diesel

blend as a fuel. International Journal of Automotive and Mechanical Engineering. 2015;11:2199-211.
[9] Rashidi M. Calculation of equilibrium composition in combustion products. Chemical Engineering and Technology. 1997;20:571-5.
[10] Way R. Methods for determination of composition and thermodynamic properties of combustion products for internal combustion engine calculations. Proceedings of the Institution of Mechanical Engineers. 1976;190:687-97.
[11] Ramachandran S. Rapid thermodynamic simulation model of an internal combustion engine on alternate fuels. Proceedings of the International MultiConference of Engineers and Computer Scientists. 2009. p. 18-20.
[12] Heywood JB. Internal combustion engine fundamentals: Mcgraw-hill New York;1988.
[13] Gonca G. Investigation of the influences of steam injection on the equilibrium combustion products and thermodynamic properties of bio fuels (biodiesels and alcohols). Fuel. 2015;144:244-58.
[14] Ngayihi Abbe CV, Danwe R, Nzengwa R. Comparative numerical study of four biodiesel surrogates for application on diesel 0D phenomenological modeling. Journal of Combustion. 2016;2016.
[15] Kayadelen HK, Ust Y. Prediction of equilibrium products and thermodynamic properties in H_2O injected combustion for $C_\alpha H_\beta O_\gamma N_\delta$ type fuels. Fuel. 2013;113:389-401.
[16] Rakopoulos C, Rakopoulos D, Kyritsis D. Development and validation of a comprehensive two-zone model for combustion and emissions formation in a diesel engine. International Journal of Energy Research. 2003;27:1221-49.
[17] Diotallevi F. Development of a multi-zone model for nox formation in diesel engines. KTH Industrial Engineering and Management, Stockolm, Sweden. 2007.
[18] Mourya D, Roy V. Combustion modeling and simulation of combustion emissions for diesel engine operating on the blends of jatropha biodiesel and diesel. International Journal of Engineering Science and Technology. 2012;4(4):1373-81.
[19] Kayadelen HK. A multi-featured model for estimation of thermodynamic properties, adiabatic flame temperature and equilibrium combustion products of fuels, fuel blends, surrogates and fuel additives. Energy. 2018;143:241-56.
[20] Morley C. Gaseq, a chemical equilibrium program for windows ver. 0.79.2005.
[21] Gordon S, McBride BJ. Computer program for calculation of complex chemical equilibrium compositions and applications. Clevland, Ohio: NASA; 1994.
[22] Sun J, Caton JA, Jacobs TJ. Oxides of nitrogen emissions from biodiesel-fuelled diesel engines. Progress in Energy and Combustion Science. 2010;36:677-95.
[23] S. Awad et al. Single zone combustion modeling of biodiesel from wastes in diesel engine .Fuel 106 (2013) 558–568
[24] Ferguson CR. Internal combustion engines: applied thermosciences. New York: John Wiley; 1986.
[25] Olikara C, Borman GL. A computer program for calculating properties of equilibrium combustion products with some applications to I.C. engines. Warrendale, Pa.: Society of Automotive Engineers; 1975.
[26] Turns SR. An introduction to combustion : concepts and applications. second ed. Boston: WCB/McGraw-Hill; 2000.
[27] JANAF Thermochemical Tables, United States National Bureau of Standards Publications NSRDS-NBS 37, 1971.